Journal of Organometallic Chemistry 695 (2010) 799–803

Contents lists available at ScienceDirect

Journal of Organometallic Chemistry

journal homepage: www.elsevier.com/locate/jorganchem

Supercritical carbon dioxide in organometallic synthesis: Combination of *sc*-CO_2 with Nafion film as a novel reagent in the synthesis of ethers from hydroxymethylmetallocenes

Viatcheslav I. Sokolov *, Lev N. Nikitin, Ludmila A. Bulygina, Victor N. Khrustalev, Zoya A. Starikova, Alexei R. Khokhlov

A.N. Nesmeyanov Institute of Organoelement Compounds, Russian Academy of Sciences, 28, Vavilov St., 119991 Moscow, Russian Federation

ARTICLE INFO

Article history:
Received 30 July 2009
Received in revised form 16 November 2009
Accepted 15 December 2009
Available online 6 January 2010

Keywords:
sc-CO_2
Metallocenes
Ferrocenes
Ruthenocenes
Carbinols
Ethers

ABSTRACT

Metallocenyl carbinols $FcCH_2OH$ (**1a**) and $RcCH_2OH$ (**1b**) dissolved in *sc*-CO_2 penetrate into the acidic Nafion film under 20 MPa and 80 or 35 °C. After removal of pressure and leaving at room temperature, the crystals rapidly formed on the surface of the film, were identified as ethers $McCH_2OCH_2Mc$, Mc = Fc or Rc, by X-ray study. Mechanism of their formation is discussed.

1. Introduction

Supercritical carbon dioxide, *sc*-CO_2, one of the most usable supercritical fluids, is capable of dissolving many organic and organometallic compounds and introducing them into porous materials and also through sorption procedure into nonporous substances that founds an application for the modification of polymers [1–4]. Application of the supercritical carbon dioxide in organometallic chemistry, mostly as a reaction medium, has been pioneered by Polyakoff and co-workers [5]. However, only few cases are known wherein CO_2 participates as a reagent in chemical reactions such as the formation of carbamino acids with amines or the insertion into the metal–carbon bond [6].

2. Results and discussion

When studying the behaviour of *sc*-CO_2 against substituted ferrocenes, we recently have found that the well-formed crystals of acetylferrocene could be obtained [7]. In this paper, we wish to report on the combined action of *sc*-CO_2 and the acidic film Nafion on metallocenyl carbinols $(C_6H_5)M(C_5H_4)CH_2OH$, M = Fe (**1a**), Ru (**1b**). It is well-known [8] that these carbinols form in acidic media metallocenylcarbenium ions $Mc\text{-}CH_2^+$ **2a,b** stable in solution due to the electron-donating participation of the metallocene group in the dissipation of (+)-charge from α-carbon over the whole molecule. The Nafion film has a strong acidic character owing to sulfonic groups linked to the perfluoroalkyl radicals R^fSO_3H and might also play a role of the counter-ion. Thus it seemed to be a good candidate for forming the carbenium ions inside.

First of all, it turned out that both ferrocenylmethanol **1a** and ruthenocenylmethanol **1b** are highly soluble in *sc*-CO_2 at 20 MPa and 80 or 35 °C and after evaporation afford long needles (Fig. 1) suitable for X-ray diffraction study. Then we put in the cell a piece of Nafion film and some amount of **1a** or **1b**. On opening the cell it was found that in the former case the film became of blue-green colour (λ_{max} 620 nm) characteristic of ferricinium ion but in the last case it was coloured brown typical of carbenium ion **2b** as confirmed by UV–Vis spectra (Fig. 2). The reason for this difference is clear: ferrocene is apt to undergo one-electron oxidation to Fc^{1+} **3a** whereas only two-electron oxidation is permitted for ruthenocene, the hypothetical coloured form Rc^{1+} **3b** does not exist. In a control experiment with the *polyethylene* film, no colour was observed. The chemistry of the process can be represented by Fig. 3.

When left in air at room temperature, Nafion film did not change colour but on the smooth surface light-yellow single crystals of dissimilar appearance (comparing to **1a**) began to grow

* Corresponding author.
E-mail address: sokol@ineos.ac.ru (V.I. Sokolov).

0022-328X/$ - see front matter © 2009 Elsevier B.V. All rights reserved.
doi:10.1016/j.jorganchem.2009.12.017

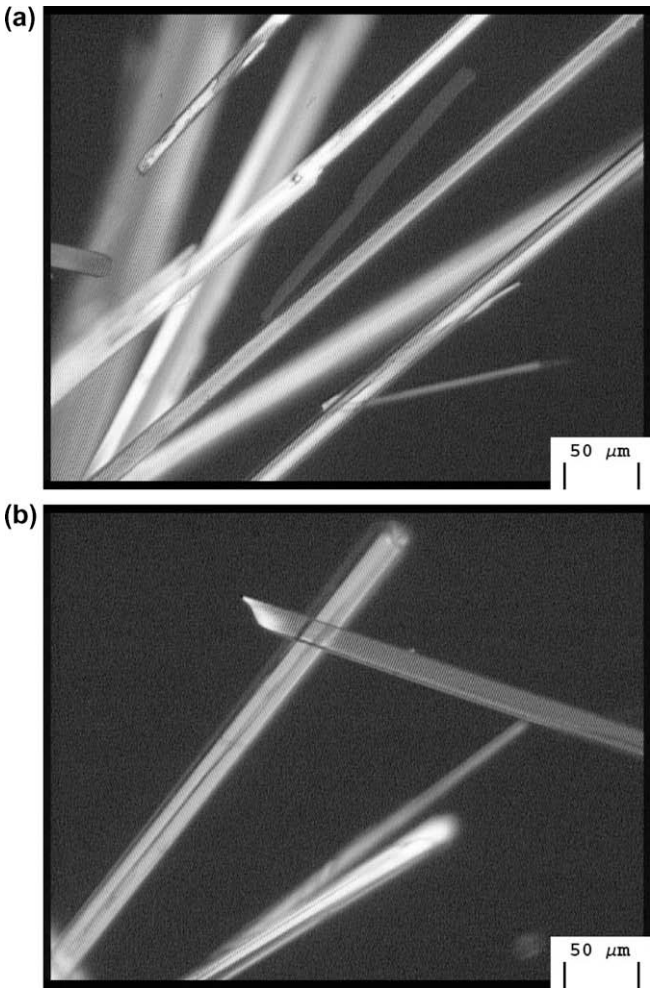

Fig. 1. Crystals of $FcCH_2OH$ (a) and $RcCH_2OH$ (b) recrystallized from *sc*-CO_2.

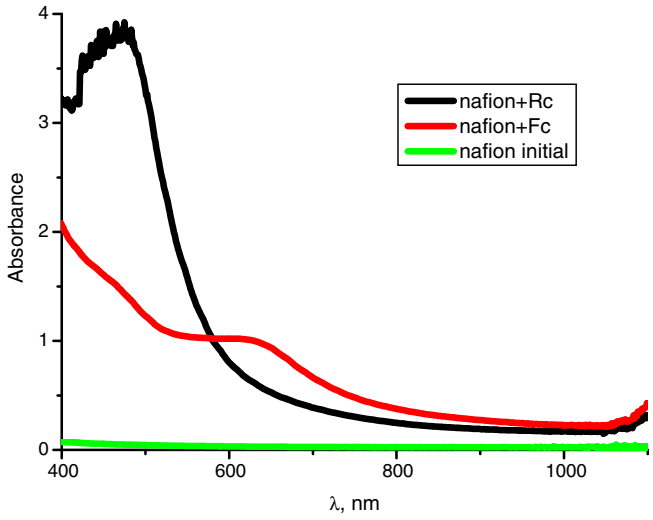

Fig. 2. UV–Vis spectra of the Nafion film: green – before reaction, red – after treatment with $FcCH_2OH$ at 80 °C and 20 MPa of *sc*-CO_2, black – after similar treatment with $RcCH_2OH$. (For interpretation of the references to colour in this figure legend, the reader is referred to the web version of this article.)

(Fig. 4) which appeared to be a known ether Fc–CH_2–O–CH_2–Fc (**4a**). Quite similarly, in the ruthenocene series the ether Rc–CH_2–O–CH_2–Rc (**4b**), hitherto unidentified, was obtained from **1b**. The

$$Fc\text{-}CH_2\text{-}OH + Fc\text{-}CH_2^+ \rightarrow Fc\text{-}CH_2\text{-}O\text{-}CH_2\text{-}Fc + H^+$$

1 a **4 a**

$$2Fc\text{-}CH_2^+ + H_2O \rightarrow Fc\text{-}CH_2\text{-}O\text{-}CH_2\text{-}Fc + 2H^+$$

$$Rc\text{-}CH_2\text{-}OH + Rc\text{-}CH_2^+ \rightarrow Rc\text{-}CH_2\text{-}O\text{-}CH_2\text{-}Rc + H^+$$

1 b **4 b**

$$2Rc\text{-}CH_2^+ + H_2O \rightarrow Rc\text{-}CH_2\text{-}O\text{-}CH_2\text{-}Rc + 2H^+$$

Fig. 3. Suggested mechanism of the formation of **4a** and **4b** from **1a** and **1b** in the acidic Nafion film.

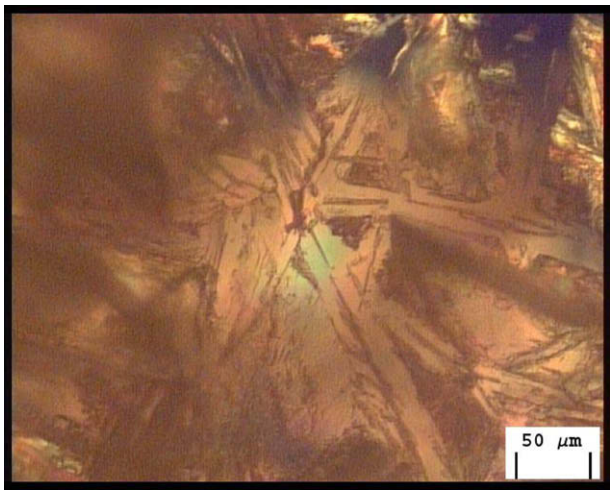

Fig. 4. Crystals of $FcCH_2OCH_2Fc$ from Nafion film + *sc*-CO_2.

whole process can be interpreted as follows. Carbinols **1a** or **1b** dissolved in *sc*-CO_2 penetrate into the Nafion film wherein carbenium ions **2a** or **2b** are formed. The natural colour of **2a** (brown as that of **2b**) is masked by the colour of a by-product **3a**. After removing the pressure carbenium ions react with the carbinol in excess under the conditions of scarcity of water (or with water itself) either inside the film or on its surface to give the corresponding ether **4a** or **4b**.

As the crystal structures of the ferrocene derivatives **1a** and **4a** were previously described [9], in the present work they were identified by the coinciding of the unit cell parameters, and the full X-ray diffraction experiments for these compounds have not been performed.

Comparison of the chemical shifts in ^1H NMR spectra of carbinols and ethers of the ferrocenyl and ruthenocenyl series is given

Table 1
Comparison of the chemical shifts in ^1H NMR spectra of carbinols and ethers of the ferrocenyl and ruthenocenyl series.

	C_5H_5	C_5H_4	CH_2	Ref.
1a	4.242 7H	4.303 (t) 2H	4.393 (s) 2H	This work and [9]
4a	4.178 (s) 5H	4.288 (t) 2H 4.215 (t) 2H	4.331 (s) 2H	This work and [9]
1b	4.681 (s) 5H	4.736 (t) 2H 4.616 (t) 2H	4.078 (s) 2H	This work
4b	4.582 7H	4.705 (t) 2H	4.164 2H	This work

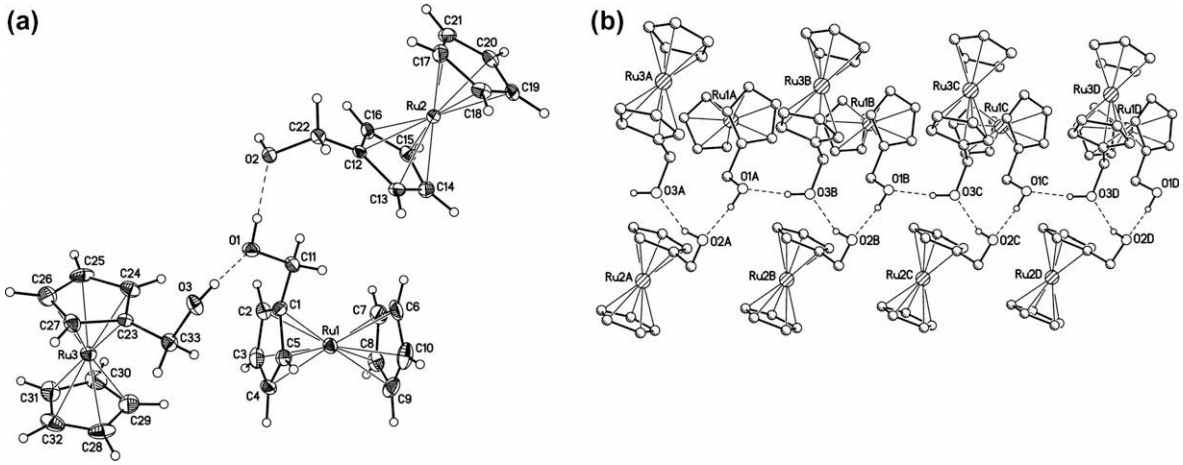

Fig. 5. Molecular structure of **1b** (ellipsoids are drawn at 50% probability). The three crystallographically independent molecules are shown. The H-bonded helicoidal chain lying along the *b*-axis direction. Hydrogen atoms, except those involved in hydrogen bonding, are omitted for clarity. The dash lines indicate the hydrogen bonds.

Table 2
Selected bond distances (Å) and bond angles (°) for **1b**.

Ru1–C(Cp)	2.148(4)–2.197(4)	C22–O2	1.440(3)
C1–C11	1.479(4)	Ru3–C(Cp)	2.155(4)–2.187(4)
C11–O1	1.440(4)	C23–C33	1.485(5)
Ru2–C(Cp)	2.163(4)–2.194(4)	C33–O3	1.445(4)
C12–C22	1.490(4)		
Ru1–C1–C11	122.7(3)	C12–C22–O2	112.5(2)
C1–C11–O1	109.5(3)	Ru3–C23–C33	125.1(2)
Ru2–C12–C22	123.4(2)	C23–C33–O3	111.4(3)

Table 3
Hydrogen bonds for **1b** [Å and °].

D–H···A[a]	*d*(D–H)[a]	*d*(H···A)[a]	*d*(D···A)[a]	∠(DHA)[a]
O1–H1O···O2	0.89	1.74	2.627(3)	173
O2–H2O···O3[b]	0.87	1.87	2.664(3)	151
O3–H3O···O1	0.88	1.81	2.678(3)	172

[a] D = donor, A = acceptor.
[b] Symmetry transformation used to generate equivalent atoms: *x*, *y* + 1, *z*.

in Table 1. Chemical shifts for **1a** and **4a** determined in this work were in agreement with those reported previously [9a,b].

Compound **1b** crystallizes in the monoclinic space group *C*2/*c* with three molecules in the asymmetric unit. The molecular structure of **1b** is shown in Fig. 5 along with the atom numbering scheme. Selected bond lengths and angles are listed in Table 2.

The geometries of the three independent molecules of **1b** are very similar to each other as well as those reported for the related compounds [10]. For example, the Ru–C distances in the three ruthenocenyl moieties fall in the range of 2.148(4)–2.197(4) Å. However, there is one striking distinction between the three unique molecules of **1b**, namely, two of the three ruthenocene fragments containing Ru1 and Ru2 have almost eclipsed cyclopentadienyl (Cp) groups, whereas the other ruthenocene fragment containing Ru3 adopts staggered conformation of Cp-groups. The largest pseudo-torsion angles determined as the angles between the C–H bond of one Cp and the C–H bond of the other Cp of the ruthenocene are 5.1°, 2.3° and 26.3°, respectively. Interestingly, the same feature has been observed in the recently reported Fe-analog **1a** [9]. Apparently, this feature is explained by the intermolecular hydrogen bonding in these compounds (Table 3). As for **1a**, each OH-group in the structure of **1b** is involved in two intermo-

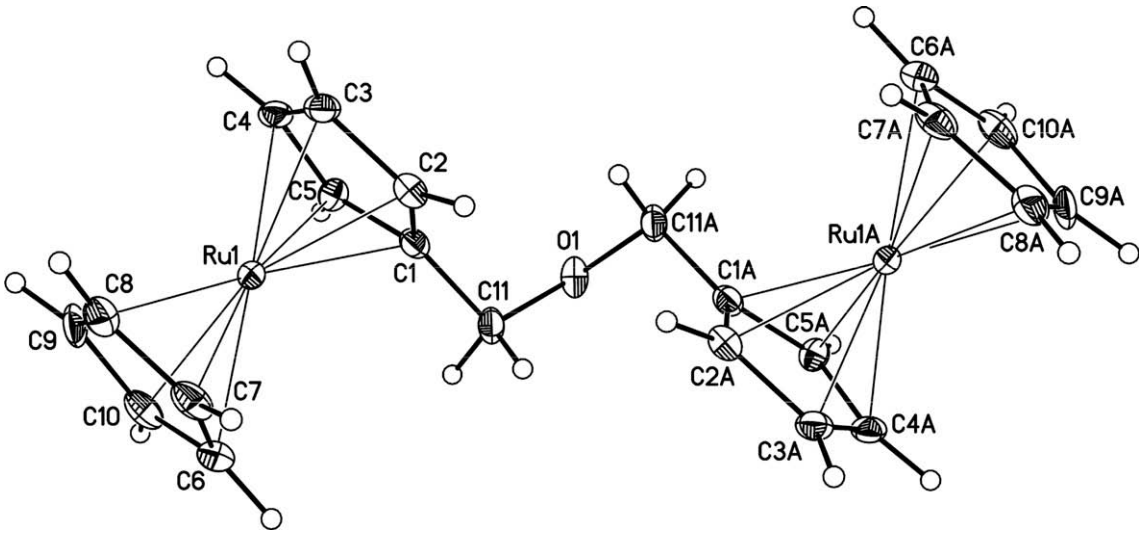

Fig. 6. Molecular structure of **4b** (ellipsoids are drawn at 50% probability). One of the two crystallographically independent molecules is shown.

Table 4
Selected bond distances (Å) and bond angles (°) for **4b**.

Ru1–C(Cp)	2.159(3)–2.191(3)	Ru2–C(Cp)	2.170(3)–2.190(3)
C1–C11	1.487(5)	C12–C22	1.490(5)
C11–O1	1.442(4)	C22–O2	1.432(4)
Ru1–C1–C11	126.3(2)	Ru2–C12–C22	126.0(2)
C1–C11–O1	111.7(3)	C12–C22–O2	112.6(2)
C11–O1–C11[a]	113.0(4)	C22–O2–C22[b]	113.4(4)

[a] Symmetry transformations used to generate equivalent atoms: $-x+3/2$, y, $-z+1/2$.
[b] Symmetry transformations used to generate equivalent atoms: $-x+1/2$, y, $-z+1/2$.

Table 5
Crystallographic data for **1b** and **4b**.

Compound	**1b**	**4b**
Empirical formula	$C_{11}H_{12}ORu$	$C_{22}H_{22}ORu$
Formula weight	261.28	504.54
Temperature (K)	120(2)	100(2)
Crystal size (mm)	0.30 × 0.03 × 0.03	0.24 × 0.12 × 0.02
Crystal system	Monoclinic	Monoclinic
Space group	*C*2/*c*	*P*2/*n*
a (Å)	44.870(5)	12.7652(12)
b (Å)	5.9408(7)	5.6624(5)
c (Å)	25.126(3)	25.065(2)
α (°)	90	90
β (°)	122.121(2)	102.080(2)
γ (°)	90	90
V (Å^3)	5672.5(11)	1771.6(3)
Z	24	4
d_c (g cm^{-3})	1.836	1.892
F(0 0 0)	3120	1000
μ (mm^{-1})	1.610	1.711
$2\theta_{max}$ (°)	60	60
Index range	$-62 \leqslant h \leqslant 62$ $-8 \leqslant k \leqslant 8$ $-35 \leqslant l \leqslant 35$	$-17 \leqslant h \leqslant 18$ $-7 \leqslant k \leqslant 7$ $-35 \leqslant l \leqslant 35$
No. of reflections collected	31 466	22 003
No. of unique reflections [$R_{(int)}$]	8237 (0.062)	5166 (0.067)
No. of reflections with $I > 2\sigma(I)$	5752	3924
Data/restraints/parameters	8237/1/352	5166/0/227
*R*1; *wR*2 ($I > 2\sigma(I)$)	0.0522; 0.1119	0.0359; 0.0614
*R*1; *wR*2 (all data)	0.0843; 0.1282	0.0592; 0.0670
Goodness-of-fit (GOF) on F^2	1.014	1.004
T_{min}; T_{max}	0.644; 0.953	0.684; 0.966

lecular hydrogen bonds, acting both as a hydrogen atom donor and acceptor. Thus, the helicoidal chains along the *b*-axis are formed, in which each hydrogen atom of the hydroxyl groups is bound to an oxygen atom of the adjacent molecule (Fig. 5). It is important to note that compound **1b** comprises both left and right-handed chains, while the non-centrosymmetric structure of **1a** (chiral space group *C*2) consists only of the left-handed chains.

Compound **4b** crystallizes in the monoclinic space group *P*2/*n* with two half-molecules in the asymmetric unit (Fig. 6). The structure is typical with all distances and angles falling in the expected range (Table 4). Nevertheless, similar to **1a** and **1b**, it is interesting to compare the structure **4b** with that of its Fe-analog **4a** [9]. Both structures are quite similar (isostructural) with the exception of slightly smaller Ru–C(Cp)–C(CH_2O) angles in **4b** (av. 126.2(2)°) compared to Fe–C(Cp)–C(CH_2O) angles in **4a** (av. 127.1(6)°). Moreover, the angles between two linked Cp rings in **4b** (av. 37.7°) are larger than those in **4a** (av. 33.5°). As for **4a**, a packing diagram of **4b** shows the alternating perpendicular and parallel orientation of the ruthenocene moieties within the crystal.

3. Conclusion

We have demonstrated here the usefulness of *sc*-CO_2 as a promoter of the reaction in the organometallic series wherein it served as a means of transportation of a reactant to the actual place wherein the reaction proceeds. Result was a targeted preparation of the metallocenyl derivatives $McCH_2OCH_2Mc$ (Mc = Fc, Rc) not easily accessible otherwise. At the same time it was shown that the Nafion film can be used as an acidic reagent for synthetic purpose in the area of organometallic chemistry.

4. Experimental

All experiments were carried out in a stainless steel 10 cm^3 cell wherein solid metallocenyl carbinol and a piece of the transparent Nafion® film (~1 cm^{-2}) were placed under 20 MPa and 35 or 80 °C for 2 h. The pressure generator (High Pressure Equipment, USA) and the cell were equipped with mechanical manometers for pressure control and with a system of valves for CO_2 inlet and depressurization. The temperatures was maintained with an accuracy of at least ±0.5 °C. The pressure in the cell was maintained with an accuracy of ±0.2 MPa. Depressurization was done using a fine-adjustment needle valve over a period of 10 min. After crystallization, crystals was obtained as light-yellow or white single crystals (Fig. 1b and c), which were analyzed using an Axiolab Pol (Zeiss) polarization microscope with crossed and non-crossed polaroids. The presence of the finely disperse phase can indicate good crystals solubility in supercritical CO_2 under the experimental conditions.

^{1}H NMR spectra were registered using spectrometer Bruker Avance-300 in $CDCl_3$. Chemical shifts were measured relative to TMS.

4.1. Preparation of bis(metallocenylmethyl) ethers 4a and 4b

In a representative experiment, Nafion film (60 mg) and $FcCH_2OH$, **1a**, (12 mg) were taken, reacted under 20 MPa and 80 °C. After opening the cell weight of the film was 64.5 mg, that means ~7.5% w/w was absorbed and then afforded crystals of the known *bis*(ferrocenylmethyl)ether **4a**.

The new *bis*(ruthenocenylmethyl)ether was obtained similarly and characterized by X-ray study and ^{1}H NMR spectrum (see Table 1).

4.2. X-ray crystal structures of compounds 1b and 4b

Data were collected on a Bruker SMART 1K CCD (for **1b**) and a Bruker SMART APEX II CCD (for **4b**) diffractometers (λ(Mo Kα)-radiation, graphite monochromator, ω and φ scan mode) and corrected for absorption using the SADABS program (versions 2.01 [11] for **1b** and 2.03 [12] for **4b**). For details see Table 5. The structures were solved by direct methods and refined by full-matrix least squares technique on F^2 with anisotropic displacement parameters for non-hydrogen atoms. The hydrogen atom of the OH-group in **1b** was localized in the difference-Fourier syntheses and included in the refinement with fixed positional and isotropic displacement (U_{iso}(H) = 1.2 U_{eq}(O)) parameters. The other hydrogen atoms in both compounds were placed in calculated positions and refined within the riding model with fixed isotropic displacement parameters (U_{iso}(H) = 1.2 U_{eq}(C)). All calculations were carried out using the SHELXTL program [13].

Supplementary material

CCDC 718014 and 718015 contains the supplementary crystallographic data for **1b** and **4b**. These data can be obtained free of charge from The Cambridge Crystallographic Data Centre via www.ccdc.cam.ac.uk/data_request/cif.

Acknowledgements

This work was financially supported by the Russian Foundation for Basic Research (Grants 08-03-00169, 07-03-91584, 08-03-00294 and 08-03-90012) as well as by the Russian Academy of Sciences (Program of Division of Chemistry and Material Sciences "Creation of new metallic, ceramic, glass, polymeric and composite materials").

References

[1] A. Lopez-Periago, A. Argemi, J.M. Andanson, V. Fernandez, C.A. Garcia-Gonzalez, S.G. Kazarian, J. Saurina, C. Domingo, J. Supercrit. Fluid. 48 (2009) 56–63.
[2] B.S.K. Gorle, I. Smirnova, M.A. McHugh, J. Supercrit. Fluid. 48 (2009) 85–92.
[3] T. Sakakura, J.-C. Choi, H. Yasuda, Chem. Rev. 107 (2007) 2365–2387.
[4] R.S. Oakes, A.A. Clifford, C.M. Rayner, J. Chem. Soc., Perkin Trans. 1 (2001) 917–941.
[5] J.R. Hyde, P. Licence, D. Carter, M. Polyakoff, Appl. Catal. A, Gen. 222 (1–2) (2003) 119–131.
[6] D.H. Gibson, Chem. Rev. 96 (1996) 2003–2053.
[7] V.N. Khrustalev, L.N. Nikitin, A.Yu. Vasíĺkov, A.R. Khokhlov, Russ. Chem. Bull. 55 (2006) 576–578.
[8] W.E. Watts, J. Organomet. Chem. Libr. 7 (1979) 399–423.
[9] (a) G. Gasser, A.J. Fischmann, C.M. Forsyth, L. Spiccia, J. Organomet. Chem. 692 (2007) 3835–3840. Compound **4a** has been obtained in this work as a by-product, one of three;
(b) V. Kovac, V. Rapic, I. Susnik, M. Suprina, J. Organomet. Chem. 530 (1997) 149.
[10] (a) M.I. Bruce, B.W. Skelton, R.C. Wallis, J.K. Walton, A.H. White, M.L. Williams, Chem. Commun. (1981) 428–430;
(b) I.E. Zanin, M.Yu. Antipin, Yu.T. Struchkov, Crystallogr. Rep. 36 (1991) 420–428;
(c) C.U. Beck, L.D. Field, T.W. Hambley, P.A. Humphrey, A.F. Masters, P. Turner, J. Organomet. Chem. 565 (1998) 283–296;
(d) M. Sato, Y. Kubota, Y. Kawata, T. Fujihara, K. Unoura, A. Oyama, Chem. Eur. J. 12 (2006) 2282–2292;
(e) E. Becker, V. Stingl, G. Dazinger, K. Mereiter, K. Kirchner, Organometallics 26 (2007) 1531–1535.
[11] G.M. Sheldrick, SADABS, v. 2.03, Bruker/Siemens Area Detector Absorption Correction Program, Bruker AXS, Madison, Wisconsin, 2003.
[12] G.M. Sheldrick, SADABS, v. 2.01, Bruker/Siemens Area Detector Absorption Correction Program; Bruker AXS, Madison, Wisconsin, 1998.
[13] G.M. Sheldrick, Acta Crystallogr. A 64 (2008) 112–122.